

Isothermal *in situ* reduction kinetic analysis of NiCl₂-containing gel

G C DAS, A BASUMALLICK[†], KINJALKINI BISWAS (SEN) and S MUKHERJEE

Department of Metallurgical Engineering, Jadavpur University, Calcutta 700 032, India

[†]Department of Metallurgical Engineering, Bengal Engineering College, Howrah 711 103, India

MS received 4 February 1993; revised 14 June 1993

Abstract. Isothermal *in situ* reduction kinetic study of NiCl₂-containing gel was carried out. The detailed statistical as well as reduced time analysis show that contracting geometry and nucleation and growth type of mixed mechanisms are operative. The activation energy for reduction is in the range 158–193 kJ/mol. Thermal analysis on NiCl₂-containing gel was carried out in the temperature range 800°C to 900°C.

Keywords. *In situ* reduction; isothermal kinetics; nanocomposites; sol–gel.

1. Introduction

Nanocomposites have attracted considerable attention in recent years (Chakravorty 1992) because of their interesting physical properties which arise due to the nanometric dimensions of the crystallites. It has been found that particularly glass–metal nanocomposites possess interesting electrical (Chatterjee and Chakravorty 1990), optical (Das and Chakravorty 1989) and magnetic (Dutta *et al* 1984) properties. Glass–transition metal nanocomposites are prepared through the sol–gel route by reducing transition metal chlorides dispersed in a gel matrix at high temperature either by passing hydrogen from outside (Chatterjee and Chakravorty 1989) or by hydrogen generated *in situ* (Das *et al* 1990). However, little is known about the mechanism and activation energy of the reduction of the transition metal chlorides in the gel matrix. It is worth while to study the rate of reduction in the gel matrix from the fundamental point of view of finding the mechanism and activation energy of reduction. This will further yield valuable information on the fraction of metallization as a function of temperature and time in the nanocomposite which controls the physical properties. These two aspects of reduction have been evaluated by making use of statistical as well as reduced time plot analyses. In this paper the results on the kinetics of *in situ* reduction of NiCl₂ in gel matrix along with thermal analysis of NiCl₂-containing gel are presented.

2. Experimental

A homogeneous solution of 1 ml NiCl₂ in double distilled water, containing 0.076 g of Ni⁺⁺ per ml; 50% excess glucose; 10 ml of ethyl alcohol (C₂H₅OH); and 4 ml of water was prepared. A homogeneous solution of 10 ml C₂H₅OH and 5 ml tetraethyl orthosilicate (TEOS) was also prepared. The first solution was added dropwise to the second one under continuous stirring with a magnetic stirrer. The resulting solution was left for gelling at 40 to 50°C. Base gel with the above volumes of TEOS, C₂H₅OH and 5 ml water was made under identical conditions.

Detailed differential thermal analysis (DTA) and thermogravimetric analysis (TGA) of gel containing NiCl_2 were carried out in air and in pure N_2 at 1 atmosphere.

N_2 gas was bubbled through an alkaline pyrogallol solution and then passed through a packed bed of anhydrous calcium chloride. The resulting gas, which is free of oxygen and moisture, was made to pass slowly through an impervious tube heated to a constant temperature in an electrical heating furnace. The temperature was controlled by a proportional temperature controller with an accuracy of $\pm 1^\circ\text{C}$. The constant heating zone inside the impervious tube was identified by a Chromel–alumel thermocouple. The gel sample with known amount of NiCl_2 was introduced into the constant heating zone of the tube.

During the reduction, HCl vapour is generated according to the mechanism stated below (Das *et al* 1990) and is carried away by the nitrogen gas passed continuously through the tube. The resulting gas mixture (nitrogen and HCl vapour) was made to bubble through a known volume of double distilled water contained in absorbing towers. HCl vapour was collected in water for a fixed interval of time. Then the gas mixture was collected in another set of absorbing towers for the same period of time. The pH was measured as a function of reduction time. The pH value of the solution yields the hydrogen ion concentration in the solution as a function of time. From these data and from the known amount of metallic chloride present in the starting gel, the fraction of metallic chloride reduced was calculated. This process was repeated over 800°C to 950°C .

3. Results and discussion

Figure 1 shows the typical DTA and TGA for NiCl_2 -containing gel in both N_2 and air. The following characteristics of the figure, which are in agreement with the results of Brinker *et al* (1982), are to be noted.

(i) Endothermic trough at 90°C in the DTA curve accompanied by weight loss in TGA is due to removal of water and alcohol present in the pores of the gel.

(ii) Second exothermic peak at 280°C arises from carbonization of alkoxy group, followed by oxidation.

(iii) TGA shows continuous weight loss at higher temperatures, which accounts for water loss from polycondensation of gel matrix.

It is to be noted that the characteristics of the curves are similar for both N_2 and air atmospheres. The continuous water loss at higher temperatures evident in TGA, along with water in the gel matrix and from the decomposition of glucose, provide adequate water to carry out water gas reaction to reduce NiCl_2 in the gel matrix as follows (Das *et al* 1990).

During heating at higher temperatures, glucose present in the pores of the gel breaks to form carbon and water vapour:



Carbon so generated reacts with water vapour from polycondensation of the gel and from other sources at higher temperature to form hydrogen:



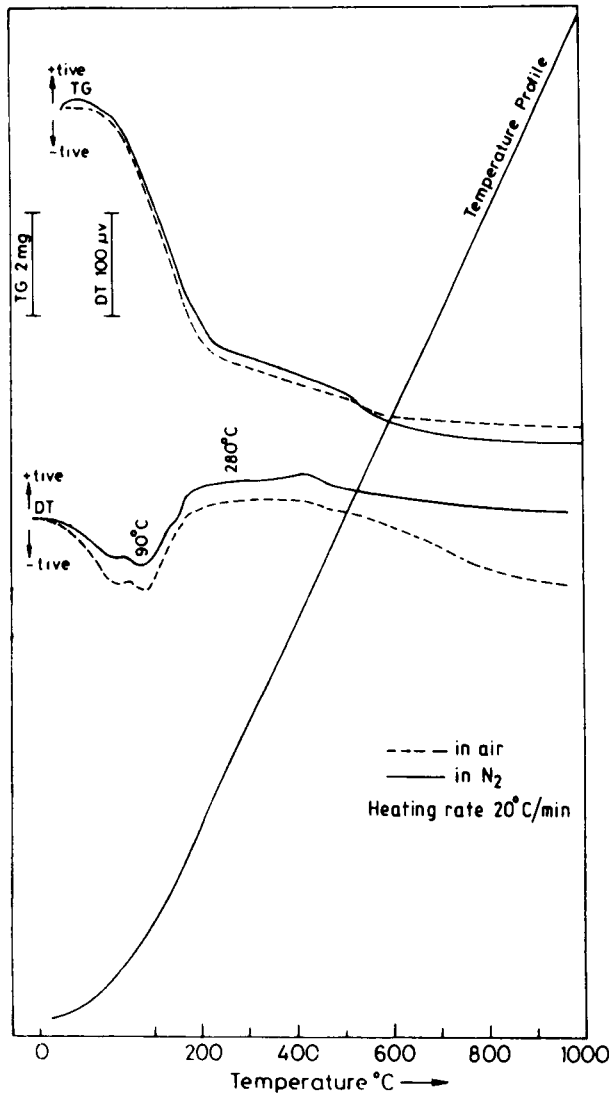


Figure 1. Thermal analysis of NiCl_2 -containing base glass.

Hydrogen so generated *in situ* reduces NiCl_2 present in the pores of the gel to form metallic nickel:



Figure 2 shows the plot of fraction of NiCl_2 converted (α) as a function of time for different temperatures. The kinetic equation is of the form $g(\alpha) = kt$, where k is the reaction rate constant. The functional form of $g(\alpha)$ depends on the mechanism. The $g(\alpha)$'s for different mechanisms are presented in table 1 (Keatch and Dollimore 1975).

The following steps are involved in statistical analysis of the kinetic data.

Step 1: For a particular mechanism and for a given temperature compute $g(\alpha)$ from α vs t plot.

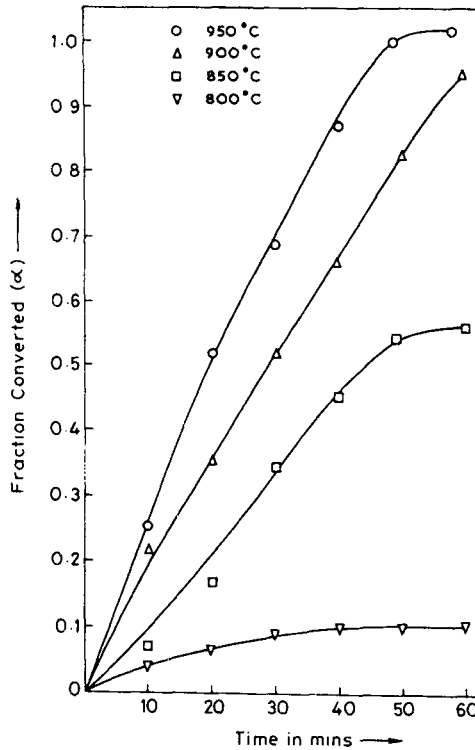


Figure 2. Plot of fraction converted (α) vs time.

Step 2: Find the goodness of fit by correlation coefficient (r)

$$r = \frac{\text{Cov}(x, y)}{\sigma_x \sigma_y}$$

$$\text{Normalized error square mean (NESM)} = \frac{\sum \{(Y_i - MX_i)/Y_i\}^2}{N}$$

Step 3: Find the slope to give k .

Step 4: Repeat steps 1 to 3 for all temperatures.

Step 5: Fit the best straight line of the type $y = Mx + c$ through $\ln k$ vs $1/T$ plot. Goodness of fit is given by correlation coefficient and NESM. Activation energy is obtained from the slope of the straight line.

Step 6: Repeat steps 1 to 5 for all mechanisms as given in table 1.

The better will be the fit the smaller the NESM and closer the value of r to unity. A computer program has been written based on the algorithm outlined above. By scanning the computer output from the point of r and NESM for all the mechanisms, we find the possible mechanism. This result is shown in table 2. We see from the table that possible mechanisms will be CG1, CG2 (contracting geometry of planar and cylindrical geometry), NG1, NG2 and NG3 (nucleation and growth types).

To reduce further the number of possible mechanisms, we have to take recourse to reduced time plot analysis. This analysis is as follows. For a particular mechanism,

$$g(\alpha) = kt. \quad (4)$$

Table 1. Mechanism for different solid state reactions.

Symbol	Name	Form of $g(\alpha)$
D ₁	Parabolic	α^2
D ₂	Valensi Barrer	$\alpha + (1 - \alpha)\ln(1 - \alpha)$
D ₃	Ginstling Brounstein	$1 - 2/3\alpha - (1 - \alpha)^{2/3}$
D ₄	Jander	$[1 - (1 - \alpha)^{1/3}]^2$
CG1	Linear growth	α
CG2	Cylindrical	$1 - (1 - \alpha)^{1/2}$
CG3	Spherical	$1 - (1 - \alpha)^{1/3}$
NG1	Avrami Erofeev	$[-\ln(1 - \alpha)]^{1/1.5}$
NG2	Avrami Erofeev	$[-\ln(1 - \alpha)]^{1/2}$
NG3	Avrami Erofeev	$[-\ln(1 - \alpha)]^{1/3}$
NG4	Avrami Erofeev	$[-\ln(1 - \alpha)]^{1/4}$
P ₁	Mampel Power	$\alpha^{1/2}$
P ₂	Mampel Power	$\alpha^{1/3}$
P ₃	Mampel Power	$\alpha^{1/4}$
R ₁	First order reaction	$[-\ln(1 - \alpha)]$
R ₂	One and half order	$[(1 - \alpha)^{-1/2} - 1]$
R ₃	Second order	$[(1 - \alpha)^{-1} - 1]$

α = Fraction reacted.

Table 2. Statistical data analysis of reduction kinetics of NiCl₂-containing gel.

Mechanism	Temp. (°C)	Correlation coefficient	NESM* $\times 10^{-2}$	Activation energy (kJ/mol)	Correlation coefficient	NESM
CG1	950	0.96	3.09	158.37	-0.93	0.0014
	900	0.99	1.22			
	850	0.97	13.64			
	800	0.91	8.71			
CG2	950	0.98	0.89	193.35	-0.95	0.0012
	900	0.98	1.36			
	850	0.98	24.58			
	800	0.91	8.50			
NG1	950	0.97	2.23	163.45	-0.98	0.0005
	900	0.97	1.92			
	850	0.98	0.82			
	800	0.90	12.00			
NG2	950	0.98	2.06	121.27	-0.98	0.0003
	900	0.98	3.76			
	850	0.97	2.82			
	800	0.90	13.90			
NG3	950	0.98	6.50	79.90	-0.98	0.0001
	900	0.99	7.90			
	850	0.96	7.90			
	800	0.90	15.70			

*Normalized error square mean.

For $\alpha = 0.5$,

$$g(0.5) = kt_{0.5}, \tag{5}$$

where $t_{0.5}$ is the time required for 50% conversion. Dividing (4) by (5), we get

$$\frac{g(\alpha)}{g(0.5)} = \frac{t}{t_{0.5}} = \theta, \tag{6}$$

where θ is the reduced time. So from (6) we see that α vs θ plot is independent of k , the reaction rate constant, which is the temperature-dependent term in kinetics. Therefore, for the same mechanism operative over the entire range of temperature, the computed α vs θ plot from experimental data will coincide with the theoretically computed α vs θ plot for the mechanism. Therefore, by comparing the computed α vs θ plot from experimental data with the theoretically computed α vs θ plot for all the mechanisms we can find out what mechanism is actually operative.

Figure 3 shows the reduced time plot for nucleation growth type of mechanisms.

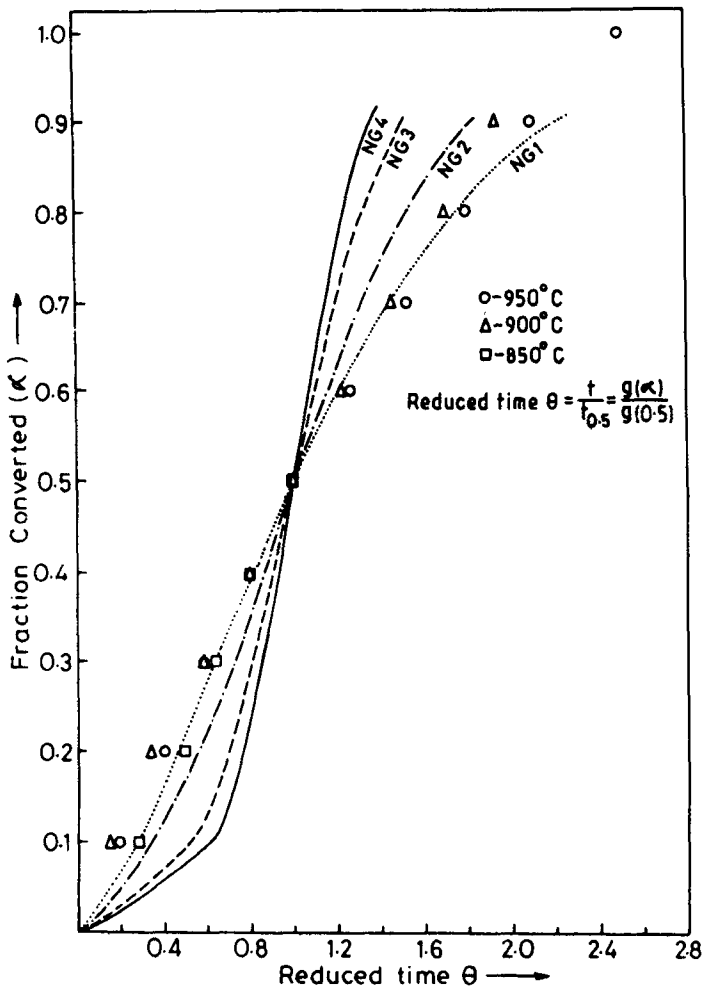


Figure 3. Plot of fraction converted (α) vs reduced time (θ).

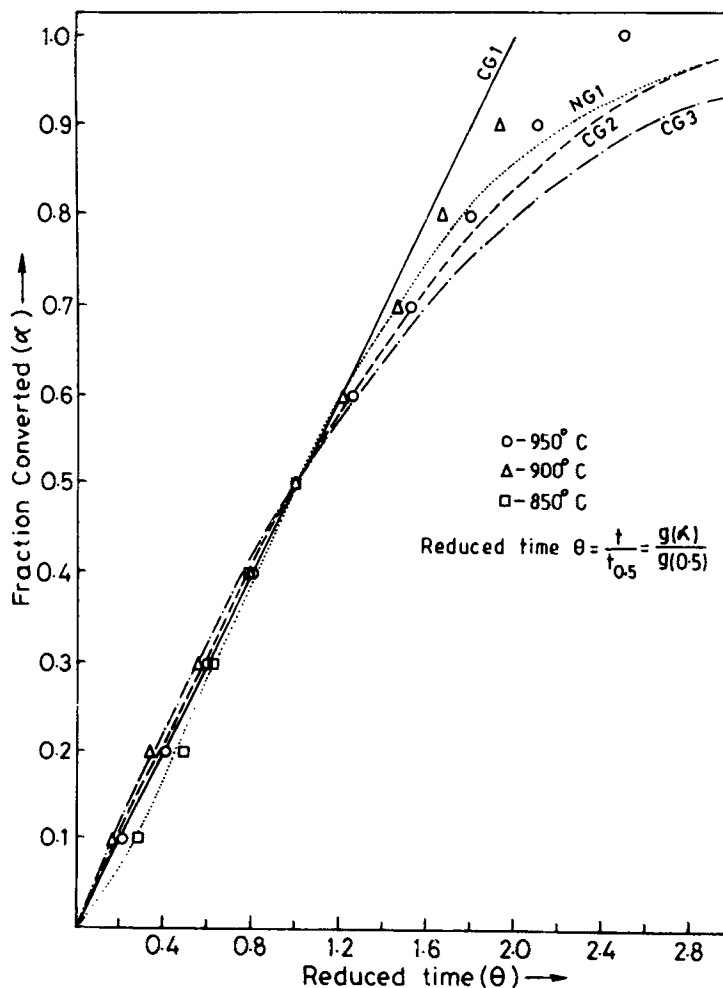


Figure 4. Plot of fraction converted (α) vs reduced time (θ).

We see that the experimentally computed values cluster around the reduced time plot curve for NG1. Therefore, of the NGs, the possible mechanism is NG1.

Figure 4 shows the comparison of experimentally computed values with the reduced time plots for CG1, CG2, CG3 and NG1. We see from the figure that the experimental points lie near CG1, CG2 and NG1. Therefore the mechanism of *in situ* reduction over the range 800–950°C is mixed CG1, CG2 and NG1. The activation energy is in the range 158 to 193 kJ/mol (see table 2). These mechanisms are consistent with physical reasoning as follows. During the course of gelling, the NiCl_2 is precipitated along the interconnected pores of the gel of dimension of a few nanometres. Therefore, it is likely that this precipitated NiCl_2 will provide a planar and cylindrical surface for reduction. Therefore the morphology of metallic Ni is expected to be flat and cylindrical. Since the boiling point of NiCl_2 is 973°C (Perry *et al* 1973), part of NiCl_2 , particularly for high temperature of reduction, e.g. 950°C (see figure 4), will be in the vapour state and reduction of NiCl_2 will occur in the vapour state. Since the melting point of Ni is 1452°C (Perry *et al* 1973), atomic Ni which is so reduced will subsequently be solidified by nucleation and growth mechanisms. Therefore NG type of mechanism

of reduction is possible. An NG type of mechanism gives spherical shape of particles. A transmission electron micrograph of this type of nanocomposite (Das et al 1990) shows the interconnected cylindrical and spherical morphology of metallic granules. Therefore it can be concluded from the above study that the mechanism of *in situ* reduction is mixed type—nucleation growth and contracting geometry.

Acknowledgement

The authors thank the Council of Scientific and Industrial Research, New Delhi, for sponsoring this research on nanocomposites.

References

- Brinker G J, Keefer K D, Schaefer D W and Ashley C S 1982 *J. Non-Cryst. Solids* **48** 47
Chakravorty D 1992 *Bull. Mater. Sci.* **15** 411
Chatterjee A and Chakravorty D 1989 *J. Phys. D. Appl. Phys.* **22** 1386
Chatterjee A and Chakravorty D 1990 *J. Phys. D. Appl. Phys.* **23** 1097
Das G C and Chakravorty D 1989 *Bull. Mater. Sci.* **12** 449
Das G C, Basumallick A and Mookherjee S 1990 *Bull. Mater. Sci.* **13** 255
Dutta S, Bahadur D and Chakravorty D 1984 *J. Phys. D. Appl. Phys.* **17** 163
Keatch C J and Dollimore D 1975 in *An introduction to thermogravimetry*, (London: Heyden and Sons Ltd) 2nd ed p. 57
Perry R H and Chilton C H 1983 *Chemical engineer's handbook*, (Tokyo: Kogakusha Ltd.) pp. 3–17